Direct Numerical Simulation and PIV Measurement of Turbulent Boundary Layer over a Rod-Roughened Wall

Seung-Hyun Lee, Jae Hwa Lee, and Hyung Jin Sung

Abstract The effects of surface roughness on a spatially-developing turbulent boundary layer were investigated by performing direct numerical simulation and particle image velocimetry measurements of TBLs over rough and smooth walls. Introduction of the roughness elements augmented turbulent stresses in the region of $y < 4 \sim 5k_s$, where k_s is an effective sand roughness height. However, the roughness has little effect on the vorticity fluctuations, turbulent kinetic energy budget and quadratic components of Reynolds shear stress in the outer layer. We also demonstrate the modification of coherent vortical structures over the rod-roughened wall by using linear stochastic estimation.

1 Introduction

Turbulent boundary layers (TBLs) are observed in numerous fluid dynamic engineering applications, and the characteristics of TBLs have been examined in many experimental and numerical studies. In real engineering applications involving wall-bounded boundary layer flow, the roughness of the wall surface is an important design parameter because it influences characteristics such as the transport of heat, mass and momentum. Although the effects of surface roughness on a TBL have been examined in many experimental and numerical studies, knowledge of these effects remains incomplete.

Townsend [1]'s Reynolds number similarity hypothesis and subsequent extensions by Jimenez [2] state that outside the roughness sublayer turbulent motions are independent of the surface roughness, and that the interaction between the inner and outer layers is very weak at sufficiently large values of the Reynolds number

S.-H. Lee, J.H. Lee, and H.J. Sung (✉)
Department of Mechanical Engineering, Korea Advanced Institute of Science and Technology (KAIST), 373-1, Guseong-dong, Yuseong-Gu, Daejeon, 305-701, Korea
e-mail: leehuiso@kaist.ac.kr; jhlee06@kaist.ac.kr; hjsung@kaist.ac.kr

T.B. Nickels (ed.), *IUTAM Symposium on The Physics of Wall-Bounded Turbulent Flows on Rough Walls*, IUTAM Bookseries 22, DOI 10.1007/978-90-481-9631-9_1,

normalized by the wall shear stress. In further support of this similarity hypothesis, a number of studies have found that the outer layers of flows past smooth and rough walls were similar in terms of both mean flow and turbulent statistics, consistent with Townsend's hypothesis for three-dimensional roughness. These studies include the work of Shockling et al. [3] on a honed pipe, and the examination of sandpaper and a woven mesh by Flack et al. [4]. Results from several experimental studies of TBLs over surfaces with two-dimensional rod-roughness, however, have been contrary to the wall similarity hypothesis. For example, in experiments on TBLs over woven mesh, transverse round rod roughness elements, Krogstad and Antonia [5,6] found that introduction of roughness caused significant changes of the turbulent statistics not only in the roughness sublayer but also in the outer layer and that the interaction between the inner and outer layers was non-negligible. These experimental results oppose the notion that the outer layer of a TBL is insensitive to the surface roughness, and have led to considerable uncertainty regarding the effects of surface roughness on TBLs.

Recently, several DNS studies have been conducted to investigate the roughness effects on turbulence structures for the turbulent channel flow with rough walls because of high resolution compared to those of experimental data. Ikeda and Durbin [7] investigated the effects of surface roughness and found that two-dimensional rod roughness produces three-dimensional unorganized motions of vortices. They proposed that non-periodic and irregular spanwise vortex shedding serves as energy sources for the turbulent kinetic energy flux towards the wall surface. Coceal et al. [8] investigated coherent structures in the log region by using two-point correlations, quadrant analysis and linear stochastic estimation (LSE). They found the presence of low-momentum regions (LMRs) and hairpin-like vortices. However, since it is known that surface roughness effects are influenced by the flow type, e.g., symmetric channel flow, asymmetric channel flow, boundary layer and so on [9], it is needed to investigate the modification of coherent structure in the turbulent boundary layer with rough wall.

In the present study, the interaction between the inner and outer layers induced by rod roughness was examined through analysis of the DNS and PIV data of Lee and Sung [10] and Lee et al. [11]. The roughness was composed of two-dimensional spanwise rods with square cross-section that were periodically arranged in the streamwise direction with a pitch of $\lambda/k = 8$ in which has a maximum value of form drag [12]. To examine the outer-layer similarity and the scaling parameters, Reynolds stresses, anisotropic tensors, velocity triple product and vorticity fluctuations were investigated and quadrant analysis was performed. Further, to elucidate the redistribution of turbulent kinetic energy, we examined the pressure-strain tensors in the transport equations of the Reynolds stresses. Finally, two-point correlations, joint weighted probability density function, linear stochastic estimation and instantaneous flow fields were scrutinized to analyze the turbulent structures arising from surface roughness not only in the roughness sublayer but also in the outer layer.

2 Results

Figures 1 and 2 show a schematic of the two-dimensional rod roughness used in the present study. The roughness elements used are periodically arranged two-dimensional spanwise rods, and the roughness height is $k/\delta = 0.05$ and 0.025 where δ is the boundary layer thickness, respectively. The Reynolds number based on the momentum thickness is varied in the range $\mathrm{Re}_\theta = 300 \sim 1{,}400$ and $\mathrm{Re}_\theta = 1{,}000 \sim 1{,}500$. Recently, Lee and Sung [10] first carried out direct numerical simulation (DNS) of TBLs with rough and smooth walls and showed that the introduction of the roughness elements affected the turbulent stress not only in the roughness sublayer ($y < 5k$) but also in the outer layer ($y > 5k$). However, the roughness had

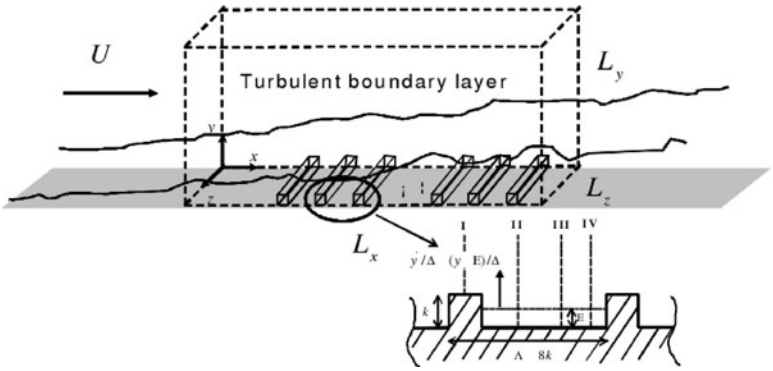

Fig. 1 Schematic of computational domain and rod roughness

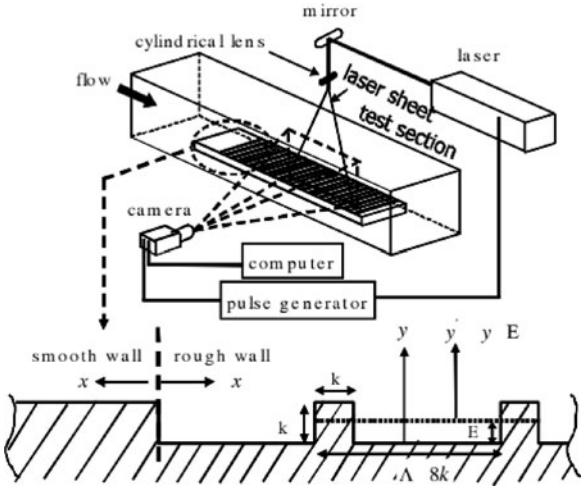

Fig. 2 Schematic of experimental arrangement and rod roughness

only a relatively small effect on the anisotropic Reynolds stress tensor in the outer layer. Despite of the first attempt of DNS in the rough-wall turbulent boundary layer, the ratio of the boundary layer thickness to the roughness height (k/δ) used in their DNS study was 0.05 and this is two times larger than the criterion of Jimenez [2] ($k/\delta \leq 0.025$). Because additional numerical simulation with smaller value of k/δ is computationally very expensive, Lee et al. [11] carried out experimental measurements to compensate the results of DNS with sufficiently small rod roughness ($k/\delta = 0.025$) by using particle image velocimetry (PIV) and showed that the introduction of the roughness elements augmented turbulent stresses in the region of $y < 4 \sim 5k_s$, where k_s is an effective sand roughness height, indicating that the effective sand roughness height is a more appropriate length scale for representing the extent of roughness effect rather than the roughness height (k).

Furthermore, Lee and Sung [10] found that when turbulent quantities are normalized by the friction velocity, rod roughness influences turbulent stresses and vertical turbulent transport not only in the roughness sublayer but also in the outer layer. However, they observed good wall similarity for the third-order moments and the Reynolds anisotropic tensor without using the friction velocity. Figure 3 shows the distributions of the r.m.s. vorticity fluctuations normalized by the friction velocity for the rough and smooth walls in the outer coordinates. Above the region $y/\delta = 0.55$ ($y \sim 11k$ and $y \sim 2k_s$), the vorticity fluctuations of the rough and smooth walls collapse well and attain the same magnitude. This indicates that above the roughness region, the small-scale structures of the vortical motions are almost the same over the rough and smooth walls. In the roughness sublayer, however, the presence of the rod roughness causes the maximum values of the three components to be smaller for the rough wall than for the smooth wall. These findings demonstrate that in the

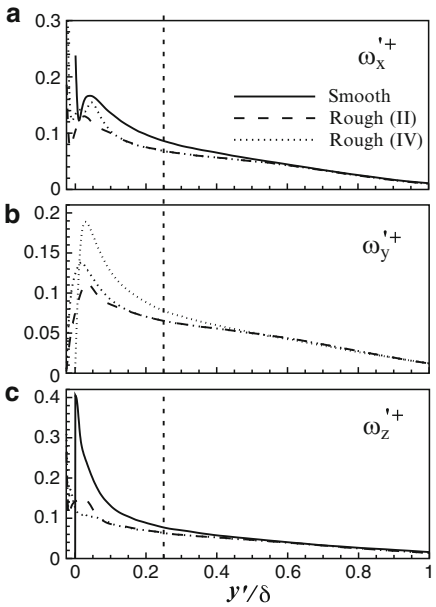

Fig. 3 Vorticity fluctuations scaled by $u_\tau{}^2/\nu$

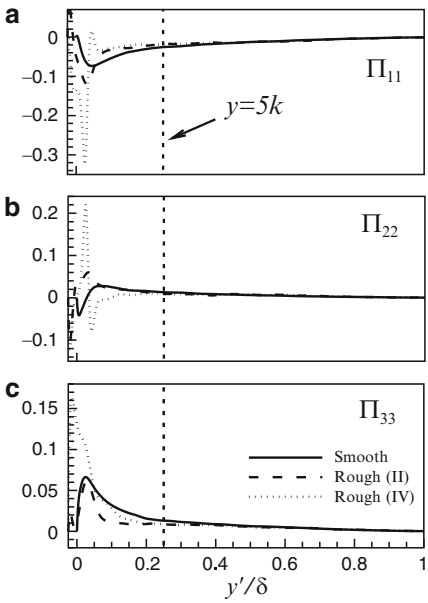

Fig. 4 Pressure-strain tensors scaled by $u_\tau{}^4/\nu$

flow past a smooth wall, in which large-scale vortices dominate, anisotropy arises rapidly and hence the vorticity fluctuations are larger in magnitude. From above results, the wall-similarity hypothesis in the outer layer depends on which turbulent statistics and scaling parameter are used in the analysis.

Lee and Sung [10] proposed that the increased production of turbulent kinetic energy in the vicinity of the rough wall causes an increase in magnitude of the turbulent Reynolds stresses, but it makes no significant contribution to the relative magnitude to the each turbulent Reynolds stress components. To better comprehend the redistribution of turbulent energy, the pressure-strain tensors in the Reynolds stress budget equation is scrutinized in Fig. 4. We can observe no discernible difference in the outer coordinates between the rough and smooth walls above $y/\delta = 0.45$ ($y \sim 9k$ and $y \sim 1.5k_s$), indicating that the redistribution of turbulent kinetic energy in the outer layer is similar in the smooth and rough walls. This finding supports the conjecture of Lee and Sung [10] that rod roughness does not significantly affect anisotropy tensors in the outer layer. Within the roughness sublayer, the turbulent energy is redistributed from $<u^{+2}>$ to $<v^{+2}>$ and $<w^{+2}>$, and the energy transfer follows a trend similar to that observed for the smooth wall, except that its magnitude is increased to a greater degree in the roughness sublayer than in the layer adjacent to the smooth wall.

To inspect the turbulent structure in the vicinity of the rough wall, quadrant components of Reynolds shear stress over the rough wall (II and IV) and one over the smooth wall are compared. Good agreement is observed in Fig. 5 between the smooth and rough walls for both the Q2 and Q4 events above $y/\delta = 0.16$ ($y \sim 3k$ and $y \sim k_s$), which is consistent with the Reynolds anisotropic tensors. These results are

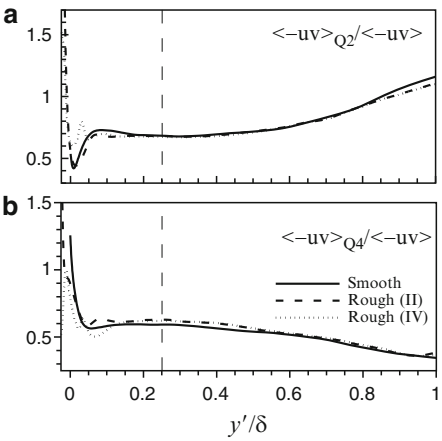

Fig. 5 Quadrant analysis scaled by local mean

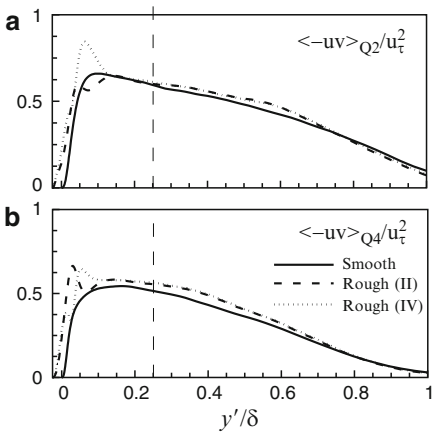

Fig. 6 Quadrant analysis scaled by $u_\tau{}^2$

consistent with those of Schultz and Flack [13], which showed outer layer similarity for three-dimensional roughness in the form of a honed pipe by investigating the percentage contributions from the ejection and sweep events. In the present study, despite the use of a roughness height of $\delta/k = 20$ ($\delta/k_s = 3.2$), good wall similarity is observed for the contributions of the Q2 and Q4 events in the outer layer for the smooth and rough walls when these variables are normalized by the local Reynolds shear stress. However, when scaled by the friction velocity, the contributions of the Q2 and Q4 events to the Reynolds shear stress in the outer layer differ markedly between the smooth and rough-walled systems (Fig. 6). This behavior is similar to that found in other experiments on TBLs over rough walls. Krogstad and Antonia [15] observed that for most of the boundary layer, the magnitudes of the Q2 and Q4 events are larger across the whole boundary layer for a woven mesh roughness of roughness height $\delta/k_s = 15$ than for the smooth wall. These findings indicate

that although the magnitudes of the Q2 and Q4 events vary not only in the roughness sublayer but also in the outer layer, the relative contributions from ejection and sweep motions in the outer layer are similar for the smooth and rough-walled systems, as was observed for the Reynolds anisotropic tensor.

The presence of rod roughness on the surface induces substantial changes in the flow field not only within the cavities between consecutive rods, but also in a certain layer above the crests of the rods. These effects can be attributed to the vigorous ejection and sweep motions that occur in these systems, as observed in the quadrant analysis. The instantaneous flow fields within the roughness sublayer reveal the characteristics of the turbulent structure over the rough wall. Figure 7 shows a visualization of the vortical structures near the roughness sublayer. The Galilean decomposition technique is applied to instantaneous velocity vectors with the reference velocity $U_f = 0.4U_\infty$ in Fig. 9b [14]. Vortical structures are identified by a positive value of the swirling strength λ_{ci} [15]. Figure 7a shows instantaneous velocity vectors (u,v) in the (x,y)-plane through the middle of the spanwise computational domain, while Fig. 7b shows the corresponding vector field of velocity fluctuations and iso-contours of vortical structures with the reference velocity $U_f = 0.4U_\infty$ in the roughness sublayer. Kline and Robinson [16] defined a vortex as a region of concentrated vorticity around which the pattern of streamlines is roughly circular when viewed in a frame moving with the centre of the vortex. Following this definition, a pattern of nearly circular streamlines that coincides with the concentrated vorticity can be discerned in Fig. 7b. The downstream regions colored light blue also

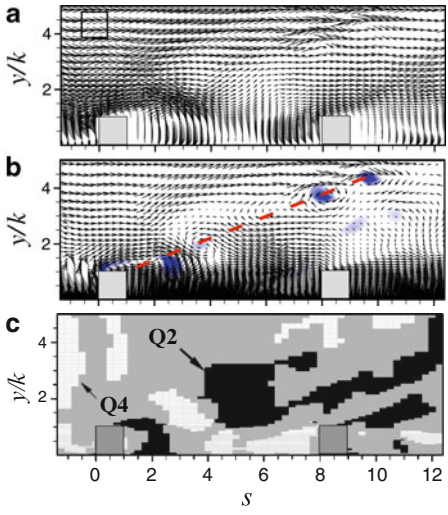

Fig. 7 Visualization of vortical structures near the roughness sublayer: (**a**) instantaneous velocity vector field of (u,v) near the roughness sublayer, (**b**) instantaneous velocity vector field with the reference frame velocity $U_f = 0.4U_\infty$ iso-contour represents the swirling strength and (**c**) spatial distribution of the Q2 and Q4 events for the same instantaneous flow field. *White* and *black regions* represent Q2 and Q4 events, respectively

contain concentrated vorticity, but their vector pattern shows only a faint circular signature because of different convection velocities. These vortices are inclined at approximately $25 \sim 26°$ with respect to the downstream direction. Adrian et al. [14] observed that in the TBL over a smooth wall, large-scale structures like hairpin packets grow upwards at a mean angle of approximately 12° as they move downstream. In similar experiments, Volino et al. [17] found angles of $13.2 \pm 2.5°$ and $15.8 \pm 3.3°$ for smooth and rough walls, respectively. A time sequence of the instantaneous flow fields shows highly disrupted vortical structures above the roughness crest, and that these structures recover rapidly with moving upwards away from the rod roughness and attain a coherence similar to that observed for the smooth wall. Figure 7c shows the spatial distributions of the Q2 and Q4 events for the same instantaneous vector field, where the Q2 and Q4 events are indicated by red and blue colors, respectively. Consistent with Coceal et al. [8], the Q2 and Q4 events are not randomly distributed but rather are grouped into distinct regions. These results indicate that large amounts of high speed fluid inrush toward the cavity region between consecutive rods, and that strong ejection motions occur near the leading edge.

Figure 8 illustrates the contours of the streamwise velocity fluctuations at $y^+ = 5$ for flows past a rough wall (top) and smooth wall (bottom). In this figure, a blue color indicates positive velocity fluctuations. At $y^+ = 5$, the streaks are elongated on the smooth wall, indicating a coherent organized structure of low speed streaks, whereas at the same wall-normal location the streaks look significantly different above the rough wall. Ashrafian et al. [18] observed streaky structures in the distribution of streamwise velocity fluctuations over the rough wall, similar to those

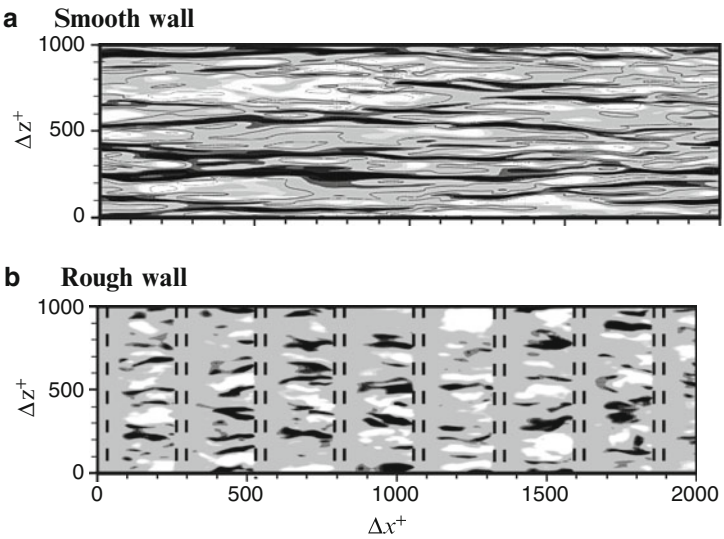

Fig. 8 Contours of streamwise velocity fluctuation at $y^+ = 5$ on the smooth wall (**a**) and rough wall (**b**). *White* and *black regions* represent high-speed ($u' > 0$) and low-speed ($u' < 0$) streaks, respectively

of the smooth wall, but with significantly reduced coherence in the streamwise direction and no obvious spanwise coherence.

To better comprehend the modification of the flow structures to Reynolds stress-producing events, we examined the conditionally averaged flow field around these structures by using linear stochastic estimation (LSE) [19]. Near-wall vortical structures are represented by plotting iso-surfaces of the swirling strength, λ_{ci} [15]. Figures 9 and 10 represent the iso-surfaces of λ_{ci} computed from the conditionally averaged velocity field of the Reynolds stress maximizing the Q2 event specified at different y locations ($y^+ = 50$ and $y/\delta = 0.5$) over rough and smooth walls. In the roughness sublayer, the streamwise vortical structures are shortened along

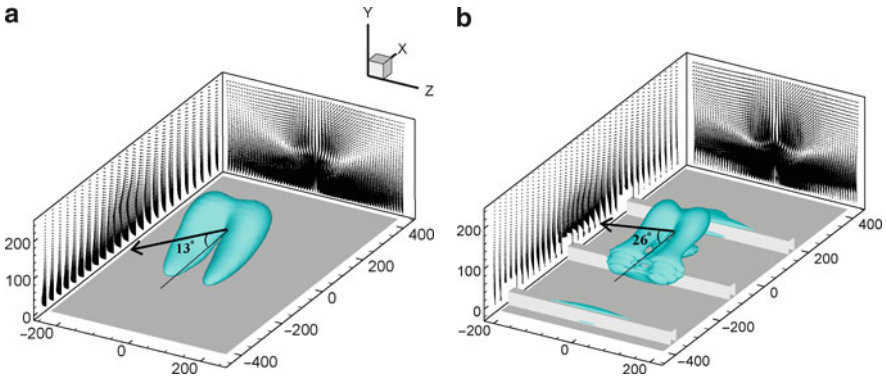

Fig. 9 Conditionally averaged vortical structure and velocity vectors fields extracted from a Q2 event maximizing the Reynolds shear stress at location II and $y^+_{ref} = 50$. Iso-surface represents λ_{ci} with the 30% contour level of the maximum value. The velocity vectors show the conditionally averaged in-plane velocity fluctuations: (**a**) smooth wall, (**b**) rough wall

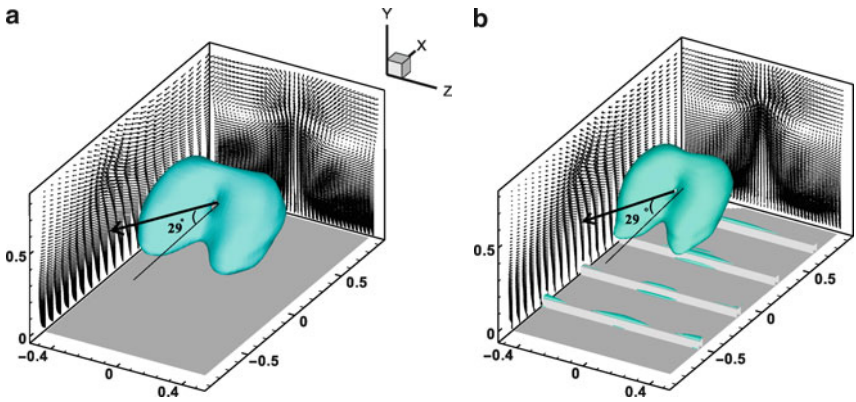

Fig. 10 Conditionally averaged vortical structure and velocity vectors fields extracted from a Q2 event maximizing the Reynolds shear stress at location II and $y_{ref}/\delta = 0.5$. Other conditions are the same as in Fig. 9: (**a**) smooth wall, (**b**) rough wall

streamwise direction and the inclination angle is increased due to the surface roughness. Above the roughness sublayer, however, the characteristics of the velocity field and swirling strength of the rough wall are similar to those of the smooth wall. This is consistent with the experimental data of Volino et al. [17], who demonstrated that the two-point correlations of various quantities and average angles of maximum correlation are in quantitative agreement between the smooth and rough wall systems in the outer layer. These findings indicate that turbulent vortices producing Reynolds stress in the outer layer of the rough wall system have almost the same geometrical shape as those in the smooth wall system.

3 Conclusions and Outlook

The effects of surface roughness on a spatially-developing TBL were investigated by performing DNS and PIV measurements of TBLs over rough and smooth walls. Emphasis was placed on the interaction between the inner and outer layers induced by the surface roughness. Despite the roughness-induced increase of the turbulent Reynolds stress tensors in the outer layer, we can observe no discernible differences of redistribution of the turbulent kinetic energy, quadratic components of Reynolds shear stress and vortical structures in the outer layer between smooth and rough walls. These findings illustrate that introduction of surface roughness elements onto the smooth surface did not significantly affect the turbulence structure in the outer layer.

References

1. A.A. Townsend, The structure of turbulent shear flow (Cambridge University Press, Cambridge, 1976).
2. J. Jimenez, Turbulent flows over rough walls. Annu. Rev. Fluid Mech. **36**, 173–196 (2004).
3. M.A. Shockling, J.J. Allen, A.J. Smits, Roughness effects in turbulent pipe flow. J. Fluid Mech. **564**, 267–285 (2006).
4. K.A. Flack, M.P. Schultz, T.A. Shapiro, Experimental support for Townsend's Reynolds number similarity hypothesis on rough walls. Phys. Fluids **17**, Article #035102 (2005).
5. P.-Å. Krogstad, R.A. Antonia, Comparison between rough- and smooth-wall turbulent boundary layers. J. Fluid Mech. **245**, 599–617 (1992).
6. P.-Å. Krogstad, R.A. Antonia, Structure of turbulent boundary layers on smooth and rough walls. J. Fluid Mech. **277**, 1–21 (1994).
7. T. Ikeda, P.A. Durbin, Direct simulations of a rough-wall channel flow. J. Fluid Mech. **571**, 235–263 (2007).
8. O. Coceal, A. Dobre, T.G. Thomas, Structure of turbulent flow over regular arrays of cubical roughness. J. Fluid Mech. **589**, 375–409 (2007).
9. P.-Å. Krogstad, H.I, Andersson, O.M. Bakken, A. Ashrafian, An experimental and numerical study of channel flow with rough walls. J. Fluid Mech. **530**, 327–352 (2005).
10. S.-H. Lee, H.J. Sung, Direct numerical simulation of turbulent boundary layer over a rod-roughened wall. J. Fluid Mech. **584**, 125–146 (2007).

11. S.-H. Lee, J.H. Kim, H.J. Sung, PIV measurements of turbulent boundary layer over a rod-roughened wall. Int. J. Heat Fluid Flow. **29**, 1679–1689 (2008).
12. S. Leonardi, P. Orlandi, R.J. Smalley, L. Djenidi, R.A. Antonia, Direct numerical simulations of turbulent channel flow with transverse square bars on one wall. J. Fluid Mech. **491**, 229–238 (2003).
13. M.P. Schultz, K.A. Flack, The rough-wall turbulent boundary layer from the hydraulically smooth to the fully rough regime. J. Fluid Mech. **580**, 381–405 (2007).
14. R.J. Adrian, C.D. Meinhart, C.D. Tomkins, Vortex organization in the outer region of the turbulent boundary layer. J. Fluid Mech. **422**, 1–54 (2000).
15. J. Zhou, R.J. Adrian, S. Balachandar, T.M. Kendall, Mechanisms for generating coherent packets of hairpin vortices. J. Fluid Mech. **387**, 353–396 (1999).
16. S.J. Kline, S.K. Robinson, Quasi-coherent structures in the turbulent boundary layer, Part 1: status report on a community-wide summary of the data. In Near Wall Turbulence. Proc. Zaric Meml. Conf. (ed. by S.J. Kline & N.H. Afghan), New York Hemisphere, 200–217 (1989).
17. R.J. Volino, M.P. Schultz, K.A. Flack, Turbulence structure in rough- and smooth-wall boundary layers. J. Fluid Mech. **592**, 263–293 (2007).
18. A. Ashrafian, H.I. Andersson, M. Manhart, DNS of turbulent flow in a rod-roughened channel. Int. J. Heat Fluid Flow. **25**, 373–383 (2004).
19. R.J. Adrian, Stochastic estimation of the structure of turbulent fields. In Eddy Structure Identification (ed. by J.P. Bonnet), Springer-Verlag, Berlin, 145–196 (1996).